Coupling between an incommensurate antiferromagnetic structure and a soft ferromagnet in the archetype multiferroic BiFeO₃/cobalt system

Marta Elzo,[1,2] Reda Moubah,[3] Camille Blouzon,[1,3] Maurizio Sacchi,[1] Stéphane Grenier,[2] Rachid Belkhou,[1] Sarnjeet Dhesi,[4] Dorothée Colson,[3] Felipe Torres,[5] Miguel Kiwi,[5] Michel Viret,[3,*] and Nicolas Jaouen[1]

[1]*Synchrotron SOLEIL, L'Orme des Merisiers, Saint-Aubin, Boîte Postale 48, 91192 Gif-sur-Yvette Cedex, France*

[2]*Institut Néel, CNRS et Université Joseph Fourier, Boîte Postale 166, 38042 Grenoble Cedex 9, France*

[3]*Service de Physique de l'Etat Condensé, CEA Saclay, DSM/IRAMIS/SPEC, URA CNRS 2464, 91191 Gif-sur-Yvette, France*

[4]*Diamond Light Source, Chilton, Didcot, Oxfordshire OX11 0DE, United Kingdom*

[5]*Departamento de Física, Facultad de Ciencias, Universidad de Chile, Casilla 653, Santiago, Chile 7800024*

and Centro para el Desarrollo de la Nanociencia y la Nanotecnología (CEDENNA), Avenida Ecuador 3493, Santiago, Chile 9170124

Multiferroic materials are mostly antiferromagnets, often containing incommensurate magnetic arrangements stemming from the magnetoelectric interaction. Using soft x-ray resonant magnetic scattering, we show that these long-range structures induce a magnetization wriggle in cobalt layers deposited on top of BiFeO₃ single crystals. This is understood using a simple interface exchange interactions model. It leads to the appearance of a magnetic anisotropy axis, which, in the particular BiFeO₃/Co system, can be manipulated using an electric field. More generally, it is demonstrated here that through interfacial magnetic exchange, antiferromagnets can leave an imprint revealing some of their hidden properties, thus providing much richer effects than mere exchange bias.

The bifunctionality of some multiferroic materials, which present simultaneous ferroelectric (FE) and magnetic orders, is a property of a great interest for potential new data storage applications. Indeed, controlling the magnetization of a ferromagnetic (FM) layer with electric fields via the so called "magnetoelectric coupling" interaction would allow the conception of electrically writable and magnetically readable memories. Only a very limited number of materials offer this property and so far, only one at room temperature: BiFeO₃ (BFO). This compound has been the object of an impressive surge of interest in the past ten years. In its bulk form, BiFeO₃ is ferroelectric and antiferromagnetic (AF), with a long-range cycloidal structure and a significant interaction between the two orders [1–5]. This AF state hinders its potential for magnetic storage applications, and in order to control a net magnetic moment with an electric field one has to rely on the exchange coupling at the interface with a FM layer [5–8]. Experimental signatures of magnetic coupling through a FM/AF interface generally include a change in the coercivity and a shift, or "bias," of the FM layer magnetization hysteresis loop. An overwhelming literature has emerged in which various mechanisms for this coupling have been proposed, debated, and tested [9]. Using multiferroics adds the promising possibility of coupling the effect with electrical polarization. However, many multiferroics present an AF long-range order which is at the heart of the magnetoelectric effect [10,11]. Despite the abundant literature on the subject, exchange coupling using AFs with long-range order has seldom been considered. It has only been recently shown that an exchange interaction exists in the bulk BFO/FM system [8], which manifests itself by the appearance of a uniaxial anisotropy. The anisotropy axis can in turn be changed by an electric field through the toggling of ferroelectric polarization domains in BiFeO₃. Here we demonstrate, using precise x-ray resonant magnetic scattering (XRMS) measurements, that the long-range antiferromagnetic structures in BiFeO₃ imprint the ferromagnet. We argue that the exchange interactions thus stem from this coupling.

The systems under study are BFO single crystals, grown by the floating zone technique, on which 10 nm thick Co layers were deposited either by ultrahigh vacuum evaporation or by ion sputtering. The magnetic structure of our BFO crystals has been thoroughly studied in the past [2,12] and consists of a *G*-type AF order following a 64 nm long-range cycloid, a structure originally determined using neutron diffraction on sintered samples [13,14]. Magneto-optical Kerr effect measurements have evidenced the appearance of an easy axis of magnetization in Co, which can be changed by switching the polarization direction of the BFO [8]. Although this was attributed to the influence of the AF cycloids onto the FM layer, a direct magnetic effect of the cycloid in the FM material has not been evidenced. Considering the small sample area (our crystals are around 1 mm²), soft x-ray resonant magnetic scattering using synchrotron light is the only technique with sufficient sensitivity to probe a possible noncollinearity in the ferromagnet at the interface with the underlying AF cycloids. A reflectivity configuration is ideal to probe magnetic depth profiles, but in-plane structures can also be investigated measuring off-specular scattering [15] when in the geometry of Fig. 1. The present paper is based on a set of such measurements performed at the I06 beamline [16] of the Diamond Light Source and at the Sextants beamline [17] of the Soleil synchrotron storage ring using the RASOR [18] and RESOXS [19] diffractometers.

In order to demonstrate their magnetic correlation, it is essential to analyze both the BFO and the Co magnetization. Synchrotron radiation allows us to resonantly probe the magnetic structures at the Fe and Co absorption edges. In the kinematical approximation, the detected intensity is proportional to the square modulus of the scattering form factor (f), summed over all positions of the magnetic atoms.
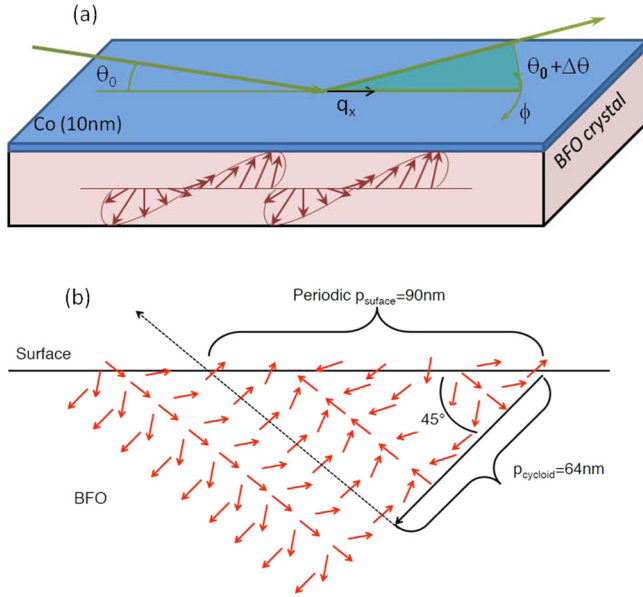
---

*michel.viret@cea.fr

FIG. 1. (Color online) (a) Schematics of the scattering geometry used in the soft x-ray experiment. The system is composed of a BFO crystal, an antiferromagnetic compound with long-range cycloids, on top of which a Co layer has been deposited. Measurements of the off-specular scattering allow us to access in-plane magnetic arrangements. (b) A cycloid in the BFO crystal impinging the [001] surface at 45° makes an interfacial 90 nm periodic structure.

Considering dipolar processes only and neglecting linear magnetic dichroism, f can be written as follows [20]:

$$\hat{f}_{e'e} = (e'^* \cdot e)F_0 - i(e'^* \times e) \cdot u F_1 + [(e'^* \cdot u)(e \cdot u)]F_2$$

with e and e' the polarization vectors of the incoming and outgoing waves, and u the unit vector along the layer magnetization. The fist term corresponds to charge scattering while the other two are the first and second order magnetic scattering. The first order in u consists of a polarization-dependent geometrical factor multiplying F_1, which is the difference between the resonant optical response of the medium for opposite magnetization-to-helicity orientations. F_1 is directly related to the observation of x-ray magnetic circular dichroism in absorption spectroscopy. We study here the resonant magnetic signal corresponding to an electric dipole transition between the $2p$ level and the d band of the Fe and Co atoms ($L_{2,3}$ edges), adding a resonant component to the scattering amplitude. In such a process, the spin-orbit interaction in the core-hole state ($2p_{1/2}$, $2p_{3/2}$) and exchange interaction in the d band act respectively as spin-dependent emitter and detector. In the scattering configuration shown in Fig. 1 the reciprocal space is scanned in the x direction with $q_x = 2\pi \sin\theta \sin\Delta\theta / \lambda$. Thus, the probed scattering vector is $q_x = k_x - k'_x$ with k_x and k'_x the x components of the wave vector of the incoming and outgoing waves. We are therefore getting information on the in-plane magnetic modulations. The reflectivity spectra at the Fe and Co L_3 edges are shown in Fig. 2 where satellites are visible on both sides of the specular reflection when at resonance. Those found at the Fe edge are expected signatures of the cycloidal AF arrangements at the BFO surface. At the Co edge, similar humps can also be seen.
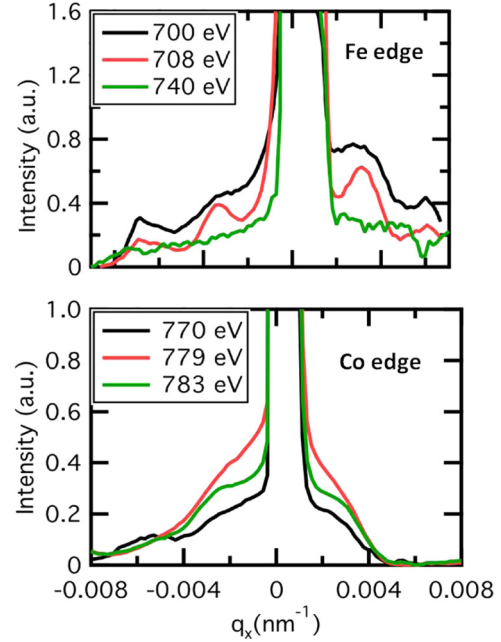

FIG. 2. (Color online) Energy dependence of the scattering spectrum around the Fe and Co edges showing the appearance of side peaks at resonance.

Although less intense, these structures unveil the existence of periodic magnetic arrangements in the thin Co layer as well. This is the central result of this paper as it directly demonstrates that the BFO cycloids imprint a long-range modulation into the adjacent ferromagnetic Co layer.

A good understanding of the position and number of the satellite peaks requires a detailed modeling of the cycloids. AF cycloids in our single electric domain BFO crystals have three symmetry-allowed propagation vectors, τ_1 [1-10], τ_2 [10-1], and τ_3 [0-11], with AF moments rotating in the planes defined by the propagation vectors and the polarization [111] direction [13]. All cycloids have a 64 nm period, but the 001 surface of our crystal cuts cycloids τ_2 and τ_3 at 45°, thus resulting in a 90 nm periodic surface structure as shown in Fig. 1. On the other hand, cycloid τ_1 which is parallel to the surface plane simply yields a 64-nm-periodic footprint. However, the measured period in Fig. 2 is around 120 nm, much larger than those expected at the surface. This can be accounted for by considering the azimuthal angle of the incident and reflected beams, which do not lay along the surface cycloidal propagation directions. Indeed, the apparent periodicity can be written as $\lambda = \lambda_0 / \cos(\phi)$ where λ_0 is the cycloid pitch in the BFO surface plane. The presence of several humps in the data indicate that the x-rays are diffracted by several cycloids with propagation vectors in different directions.

Figure 3(a) presents the results of our simulations in a polar graph representing the expected position of the off specular satellite peaks in reciprocal space as a function of the azimuthal angle. Figure 3(b) shows three sets of data taken at the Co edge at different azimuthal angles. The data points (color dots) fit very well on the modeled lines, which evidence the presence of at least two different zigzags at different positions in the sample. Indeed, for each azimuthal angle of Fig. 3 a different region is probed by the x-ray beam. Black hollow circles
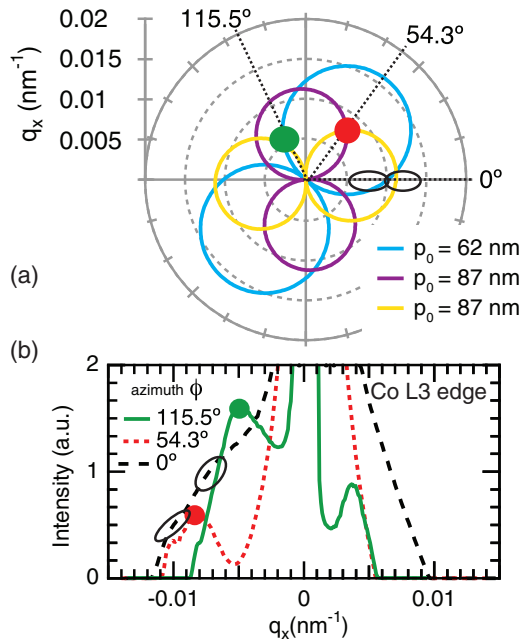
FIG. 3. (Color online) (a) Polar simulation of the satellite positions as a function of the azimuthal angle fitting very well zigzag modulations with a period of 62 nm (the dot size represents the error bars). (b) Experimental data at the Co edge for three azimuthal angles.

determined from the dashed black scattering curve belong to two different cycloids (blue and yellow in Fig. 3). The attribution of the red and green circles is not univalent: while both could belong to the same yellow cycloid, they could also pertain the former to the purple cycloid and the latter to the blue one. It therefore appears that at least two of the three symmetry-allowed cycloids in a single ferroelectric domain are present in our sample. This is in agreement with the recently reported multicycloidal domains in single ferroelectric BFO crystals [21]. Moreover, it is interesting to note that the "dead layer" evidenced in similar single crystals [22] has no incidence on the interfacial exchange. The present results directly demonstrate that the cycloids go all the way to the BFO surface.

The magnetic origin of the Co peaks is confirmed by their disappearance off-resonance and by their temperature
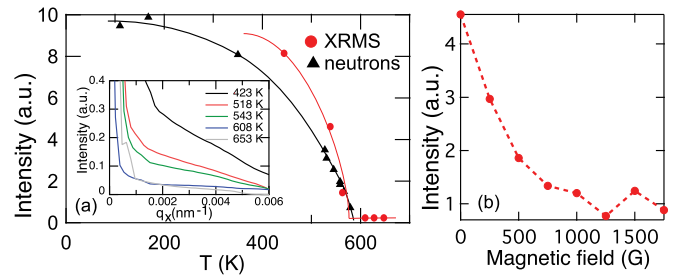

FIG. 4. (Color online) (a) Temperature dependence of the structures at the Co edge. The peaks disappear concomitantly with those at the Fe edge as temperature is raised to the Néel point of BFO. Our data are compared to neutron scattering measurements of the AF peak of BFO [23]. (b) Field dependence of the Bragg peak at the Co edge at room temperature.

dependence, as shown in Fig. 4(a) where the peak intensity at the Co L_3 edge vanishes when approaching the Néel point of BFO, in close resemblance to the intensity of the BFO AF peaks measured with neutrons [23]. To unambiguously demonstrate the magnetic origin of the Bragg peaks measured at the Co edge we report the suppression of these peaks when applying a small field of only 1500 G. This applied field is not strong enough to modify the cycloids in BFO but enough to dominate the interfacial exchange coupling at the interface. This further evidences that the ordering of the Co magnetization is driven by the presence of cycloids in BFO.

It is difficult, from our measurements alone, to provide a complete picture of the Co magnetic structure, beside its period. Magneto-optical measurements show an in-plane globally saturated Co magnetization, suggesting that the cycloid imprints manifest themselves as very small wriggles of the Co moments. It is possible to model the influence of the BFO structure in the Co using known parameters. Let us consider a rigid interface magnetization in BFO consisting of parallel linear chains oriented along the x axis with a magnetization following a cycloid. The FM overlayer is assumed magnetized in-plane. The total Hamiltonian can be written in the form of three terms representing the exchange and Zeeman energies along with an interface coupling interaction (anisotropy can be neglected):

$$\mathscr{H} = -J_{FM} \sum_{\ell=1}^{N} \sum_{\mathbf{R}} \left(\sum_{\boldsymbol{\eta}} \cos[\theta_\ell(\mathbf{R}) - \theta_\ell(\mathbf{R} + \boldsymbol{\eta})] + \cos[\theta_\ell(\mathbf{R}) - \theta_{\ell+1}(\mathbf{R})] \right)$$

$$- \mu_B g H_0 \sum_{\ell=1}^{N} \sum_{\mathbf{R}} \cos[\theta_\ell(\mathbf{R}) - \varphi_0] - J_0 \sum_{\mathbf{R}} \cos[\theta_1(\mathbf{R}) - \phi_0(\mathbf{R})],$$

where the atomic planes are indexed ℓ, starting from 0 at the BFO interface and increasing going into the Co layer, the vector $\mathbf{R}$ specifies a lattice site on the ℓth plane, and $\boldsymbol{\eta}$ is a nearest-neighbor lattice vector in this plane. The external field $\mathbf{H}_0$ is oriented in-plane and J_0 is the exchange interaction that couples Co and Fe atoms across the Co/BFO interface, while J_{FM} is the exchange interaction in the ferromagnet, the magnitude of the spin being normalized to 1. $\theta_\ell(\mathbf{R})$ is the spin angle at site $\mathbf{R}$ in the ℓth layer, φ_0 is the field angle, and

$\phi_0(\mathbf{R})$ is the canting angle at site $\mathbf{R}$ on the $\ell = 0$ Fe layer. Minimizing the energy with respect to the angle $\theta_\ell(\mathbf{r})$ at site $\mathbf{r}$ and introducing the canting angle relative to the field direction $\Theta_\ell(\mathbf{r}) = \theta_\ell(\mathbf{r}) - \varphi_0$, one obtains

$$J_{FM} \sin[\Theta_\ell(\mathbf{r}) - \Theta_\ell(\mathbf{r} + \boldsymbol{\eta})] + J_{FM} \sin[\Theta_\ell(\mathbf{r}) - \Theta_\ell(\mathbf{r} - \boldsymbol{\eta})]$$
$$+ J_{FM} \sin[\Theta_\ell(\mathbf{r}) - \Theta_{\ell+1}(\mathbf{r})] + J_{FM} \sin[\Theta_\ell(\mathbf{r}) - \Theta_{\ell-1}(\mathbf{r})]$$
$$+ \mu_B g H_0 \sin \Theta_\ell(\mathbf{r}) + \delta_{\ell,1} J_0 \sin[\Theta_1(\mathbf{r}) + \varphi_0 - \phi_0(\mathbf{r})] = 0.$$
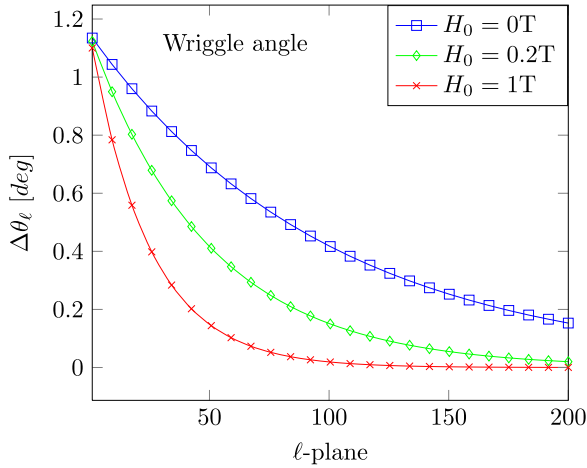
$$(1)$$

FIG. 5. (Color online) Wriggle angle in the various Co layers, as a function of the distance to the Co/BFO interface for three different values of field.

FIG. 6. (Color online) Imprinted cycloidal arrangement of the BiFeO$_3$ crystal into a wriggle in the Co layer.

Since the Co magnetization deviates only weakly from the external field, $\Theta_\ell(\mathbf{r}) \sim 0$ can be used. It is important to note here that the in-plane exchange interaction is the main term that acts to suppress the wriggle. The small oscillating component of the Co magnetization induced by the transverse component of the BFO cycloid can be decomposed in the form $\Theta_\ell(\mathbf{r} \pm \boldsymbol{\eta}) = e^{\pm i\phi(\eta)}\Theta_\ell(\mathbf{r})$, which allows one to write the deviation angle from the field direction as

$$\Theta_\ell(\mathbf{r}) = \frac{J_0\tau^\ell \sin[\phi_0(\mathbf{r}) - \varphi_0]}{J_{FM} + J_0\tau \cos[\phi_0(\mathbf{r}) - \varphi_0]} \quad (2)$$

with $\tau = \Theta_{\ell+1}(\mathbf{r})/\Theta_\ell(\mathbf{r})$. Globally this arrangement forms a zigzag following the cycloids and decaying along the direction normal to the BFO/Co interface. This variation of the full wriggle amplitude can be estimated using $\varphi_0 = 0$ and $\phi_0(\mathbf{r}) = 2\pi x/\lambda$, and it reads

$$\Delta\theta_\ell = 2\gamma_0\tau^\ell = \frac{2J_0}{J_{FM}}\left[\frac{\mu_B g H_0 + 2J_{FM}(2 - \cos\phi)}{2J_{FM}}\right.$$
$$\left. - \sqrt{\left(\frac{\mu_B g H_0 + 2J_{FM}(2 - \cos\phi)}{2J_{FM}}\right)^2 - 1}\right]^\ell. \quad (3)$$

This is represented in Fig. 5 for different values of the external field $(0, 0.2, 1)$ T, where the Co exchange energy $J_{FM} \sim 100$ meV and $J_0 \sim 10$ meV, i.e., of a similar strength as the exchange in BFO [6].
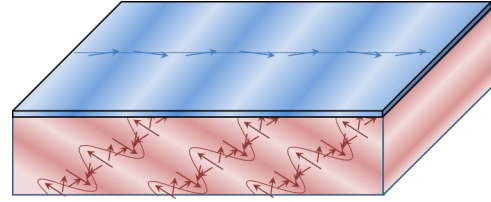
The in-plane magnetic order can also be schematized as zigzags with the same period as the surface cut of the BFO cycloid (Fig. 6). As in the case of spin waves, it appears that the system's energy is minimized when the Co magnetization is parallel to the wriggle propagation vector. For an average 1° angle, consistent with the above calculation, an anisotropy around 100 Oe can be expected, close to that measured experimentally [8]. We underline here that this is conceptually quite different from exchange bias, which is generally attributed to uncompensated spins at the interface and controlled by a field-cooling procedure. In the present case, the induced anisotropy is solely controlled by the antiferromagnetic cycloids which can be toggled by changing the electrical polarization.

In conclusion, we provide in this paper direct experimental evidence that long-range antiferromagnetic structures can be imprinted on soft ferromagnets through interface magnetic exchange. Using soft x-ray magnetic scattering reflectivity we measure the magnetic modulation in a cobalt layer deposited on multiferroic BiFeO$_3$ crystals containing antiferromagnetic cycloids. The observed magnetic wriggles are understood using a simple interfacial exchange coupling model. The propagation vectors of these structures define the anisotropy axis known to exist in soft ferromagnets deposited on BFO single crystals. We underline here that the magnetic layer could thus also be used to reveal antiferromagnetic long-range structures providing that the ferromagnet can be imaged or probed, which is usually easier than magnetic imaging in antiferromagnets.

[1] G. Catalan and J. F. Scott, Adv. Mater. **21**, 2463 (2009).

[2] D. Lebeugle, D. Colson, A. Forget, M. Viret, A. M. Bataille, and A. Goukasov, Phys. Rev. Lett. **100**, 227602 (2008).

[3] S. Lee, T. Choi, W. Ratcliff, R. Erwin, S.-W. Cheong, and V. Kiryukhin, Phys. Rev. B **78**, 100101 (2008).

[4] J. Dho, X. Qi, H. Kim, J. MacManus-Driscoll, and M. Blamire, Adv. Mater. **18**, 1445 (2006).

[5] Y. H. Chu, L. W. Martin, M. B. Holcom, M. Gajek, S. J. Han, Q. He, N. Blake, C.-H. Yang, D. Lee, W. Hu *et al.*, Nat. Mater. **7**, 678 (2008).

[6] H. Béa, M. Bibes, F. Ott, B. Dupé, X.-H. Zhu, S. Petit, S. Fusil, C. Deranlot, K. Bouzehouane, and A. Barthélémy, Phys. Rev. Lett. **100**, 017204 (2008).

[7] L. W. Martin, Y.-H. Chu, M. B. Holcomb, M. Huijben, P. Yu, S.-J. Han, D. Lee, S. X. Wang, and R. Ramesh, Nano Lett. **8**, 2050 (2008).

[8] D. Lebeugle, A. Mougin, M. Viret, D. Colson, and L. Ranno, Phys. Rev. Lett. **103**, 257601 (2009).

[9] J. Nogués and I. K. Schuller, J. Magn. Magn. Mater. **192**, 203 (1999).

[10] M. Mostovoy, Phys. Rev. Lett. **96**, 067601 (2006).

[11] H. Katsura, N. Nagaosa, and A. V. Balatsky, Phys. Rev. Lett. **95**, 057205 (2005).

[12] D. Lebeugle, D. Colson, A. Forget, M. Viret, P. Bonville, J. F. Marucco, and S. Fusil, Phys. Rev. B **76**, 024116 (2007).

[13] I. Sosnowska, T. Peterlin-Neumaier, and E. Steichele, J. Phys. C: Solid State Phys. **15**, 4835 (1982).

[14] R. Przenioslo, M. Regulski, and I. Sosnowska, J. Phys. Soc. Jpn. **75**, 084718 (2006).

[15] H. A. Durr, E. Dudzik, S. S. Dhesi, J. B. Goedkoop, G. van der Laan, M. Belakhovsky, C. Mocuta, A. Marty, and Y. Samson, Science **284**, 2166 (1999).

[16] S. S. Dhesi, S. A. Cavill, A. Potenza, H. Marchetto, R. A. Mott, P. Steadman, A. Peach, E. L. Shepherd, X. Ren, U. H. Wagner, and R. Reininger, AIP Conf. Proc. **1234**, 311 (2010).

[17] M. Sacchi, N. Jaouen, H. Popescu, R. Gaudemer, J. M. Tonnerre, S. G. Chiuzbaian, C. F. Hague, A. Delmotte, J. M. Dubuisson,

G. Cauchon, B. Lagarde, and F. Polack, J. Phys.: Conf. Ser. **425**, 072018 (2013).

[18] T. A. W. Beale, T. P. A. Hase, T. Iida, K. Endo, P. Steadman, A. R. Marshall, S. S. Dhesi, G. van der Laan, and P. D. Hatton, Rev. Sci. Instrum. **81**, 073904 (2010).

[19] N. Jaouen, J.-M. Tonnerre, G. Kapoujian, P. Taunier, J.-P. Roux, D. Raoux, and F. Sirotti, J. Synchrotron Radiat. **11**, 353 (2004).

[20] J. P. Hannon, G. T. Trammell, M. Blume, and D. Gibbs, Phys. Rev. Lett. **61**, 1245 (1988).

[21] R. D. Johnson, P. Barone, A. Bombardi, R. J. Bean, S. Picozzi, P. G. Radaelli, Y. S. Oh, S.-W. Cheong, and L. C. Chapon, Phys. Rev. Lett. **110**, 217206 (2013); **111**, 109903(E) (2013).

[22] X. Martí, P. Ferrer, J. Herrero-Albillos, J. Narvaez, V. Holy, N. Barrett, M. Alexe, and G. Catalan, Phys. Rev. Lett. **106**, 236101 (2011).

[23] P. Fischer, M. Polomska, I. Sosnowska, and M. Szymanski, J. Phys. C: Solid State Phys. **13**, 1931 (1980).